Electrostatic Evaluation of the Signature Motif (H/V)CX_5R(S/T) in Protein−Tyrosine Phosphatases[†]

Günther H. Peters,[‡] Thomas M. Frimurer, and Ole H. Olsen*

MedChem Research IV, Novo-Nordisk A/S, Novo Nordisk Park, DK-2760 Måløv, Denmark

Received May 20, 1997; Revised Manuscript Received January 6, 1998

ABSTRACT: The catalytic activity of protein−tyrosine phosphatases (PTPs) is mediated by a cysteine side chain which carries out a nucleophilic attack initiating the phosphate cleavage. Experimentally, it has been observed that the active site cysteine has a remarkably low pK_a. In the present study, we have investigated the origin of the low pK_a by analyzing the electrostatic properties of four different protein−tyrosine phosphatases: *Yersinia* PTP (bacteria), PTP1B (human), VHR (human), and low molecular weight phosphatase (bovine). These phosphatases have very low sequence homology and show very low structural similarity. However, they share a common active site motif [the (H/V)CX_5R(S/T) sequence] which adopts a unique loop structure. We have applied the so-called single site titration method, which is based on the Poisson−Boltzmann methodology, to (i) study the influence of the architecture of the (H/V)CX_5R(S/T) loop on the pK_a of the active cysteine and (ii) examine which parts of the active site region stabilize the ionized form of the cysteine. Our results indicate that the architecture of the (H/V)CX_5R(S/T) loop has a major impact on the low pK_a of the active cysteines. The orientation of the microdipoles generated by the partial charges of the backbone atoms (i.e., the $CONHC_\alpha$ atoms) is essential for maintaining the low pK_a. Further, the electrostatic field generated by these microdipoles has a larger impact than the electrostatic dipole generated by the central α-helix. Interactions of the active cysteine with other ionizable side chains play a minor role in stabilizing the thiolate anion. The only ionizable side chain significantly influencing the pK_a of the active site cysteine is the arginine, which is an important part of the consensus sequence.

Protein−tyrosine phosphorylation is a common element in signaling pathways and a key regulator of a variety of cellular events controlling, e.g., mitosis, cell proliferation, cell differentiation, and metabolism (Fisher et al., 1991; Stone & Dixon, 1994). Numerous studies have been devoted to protein−tyrosine kinases, which control the phosphorylation of tyrosine residues (Levitzki & Gazit, 1995; Rodrigues & Park, 1994; Courtneidge, 1994; Cox et al., 1994). The opposing mechanism, the dephosphorylation of tyrosines, has only recently attracted attention primarily due to the determination of three-dimensional structures of several protein−tyrosine phosphatases (PTPs) (Fauman & Saper, 1996). PTPs constitute a large diversified family of enzymes, which can be divided into two structurally distinct groups, receptor-like and soluble cytoplasmic enzymes (Saito, 1993; Pot & Dixon, 1992; Hunter, 1995).

PTPs can be identified by their sensitivity toward vanadate, the ability to hydrolyze *p*-nitrophenyl phosphate, and the complete loss of activity when the active cysteine is mutated to, e.g., serine (Zhang & Dixon, 1993). According to Fauman and Saper (1996) these phosphatases can be grouped into four families on the basis of their structure, function, and sequence: (1) the tyrosine-specific phosphatases, (2) the VH1-like dual specificity phosphatases, (3) the cdc25 phosphatases, and (4) the low molecular weight phosphatases.

A series of X-ray studies on phosphatases have revealed the structural basis of their catalytic mechanism. The three-dimensional structures of dual-specificity VHR (Yuvaniyama et al., 1996), *Yersinia* PTP (Stuckey et al., 1994; Schubert et al., 1995), low molecular weight PTP (Su et al., 1994; Zhang et al., 1994a), PTP1B (Barford et al., 1994; Jia et al., 1995) and PTPα (Bilwes et al., 1996) have been crystallographically resolved. Despite very low sequence homology, the PTPs are characterized by having an active site motif consisting of a cysteine residue and an arginine residue which are separated by five residues, the (H/V)CX_5R(S/T) motif. This conserved motif, which is referred to (in the literature) as the "P-loop", plays an important role in the binding and catalytic reaction. This loop, in combination with the arginine side chain, coordinates the oxygens of the phosphate with the main chain nitrogens and three of the arginine nitrogens. Binding of the oxyanion triggers a conformational change which brings a catalytically active aspartate (a proposed general acid) in position. Thus, the X-ray crystallographic analysis reveals that for tyrosine-specific phosphatases a conformational change is essential upon activation. The inactive conformation (the "open" conformation) exposes a large surface-accessible cleft which after the conformational change (producing the "closed" conformation) shrinks into a small pocket which binds the phosphate moiety and also a water molecule (however, the water molecule is

[†] Financial support from Danish Cancer Society (Grant 97 100 05) and Novo-Nordisk A/S (to G.H.P.) is gratefully acknowledged.

* To whom correspondence should be addressed [phone, (+45) 4443 4511; fax, (+45) 4443 4547; e-mail, oho@novo.dk].

[‡] Current address: Chemistry Department III, H. C. Ørsted Institutet, University of Copenhagen, Universitetsparken 5, DK-2100 Copenhagen Ø, Denmark.

S0006-2960(97)01187-2 CCC: $15.00
Published on Web 03/31/1998

not present in low molecular weight PTP). The reaction continues in two steps. The cysteine functions as a nucleophile and attacks the phosphorus atom in the substrate to expel the leaving phenol, resulting in the formation of a covalent thiophosphate enzyme intermediate. In the second step a water molecule attacks the phosphorus atom to yield inorganic phosphate. Experiments have shown that the pK_a of the active cysteine is unusually low (Zhang et al., 1994b), indicating that the cysteine facilitating the catalysis is negatively charged at physiological pH. It has been proposed that in *Yersinia* PTP the thiol anion is stabilized by an extensive network of hydrogen bonds between the backbone NH of the P-loop and the active cysteine (Stuckey et al., 1994; Stunnenberg, 1993). The hydrogens of the P-loop amides are all oriented toward the thiolate, suggesting that the microdipoles of the NH create an electrostatic field favoring the thiol anion (Evans et al., 1996; Stuckey et al., 1994). In the case of low molecular weight PTP and VHR no such lid motion is identified. Comparison of the solution structure (without phosphate) and the X-ray structure (complexed with phosphate) of the low molecular weight PTP shows no clear sign of a conformational change as observed for the tyrosine-specific PTPs. For VHR only the crystal structure is known, but also here an activation by a conformational change is difficult to identify.

The influence of an electrostatic field on the charge distribution has long been recognized, and it is thought that electrostatic effects play a major role in determining the structures and functions of proteins (Warshel & Åqvist, 1991; King et al., 1991; Jackson & Fersht, 1993; Honig & Nicholls, 1995). Calculations of electrostatic energies are probably the most effective way of correlating protein structures with their specific catalytic functions (Honig & Nicholls, 1995). For instance, catalysis frequently depends on the pH, i.e., on the ionization of catalytic groups (pK_a) and their electrostatic environment. Thus, one of the primary challenges in theoretical studies of protein function is the evaluation of the relevant electrostatic forces (Wells et al., 1987). This can be done effectively using macroscopic or microscopic approaches (Warshel & Åqvist, 1991) providing information about the protonation state of titratable groups (i.e., pK_as). In many biological systems, the function of proteins is frequently associated with an amino acid side chain having an unusual pK_a, e.g., in proteolytic or glycolytic enzymes (Dao-pin et al., 1991; Inoue et al., 1992; McGrath et al., 1992), in redox enzymes (Langetsmo et al., 1991a,b), in the metabolism of ATP (Auzat & Garel, 1992), in a light-driven proton pump (Khorana, 1993), in *Escherichia coli* aspartate transcarbamylase (Villoutreix et al., 1994), or in photosynthetic reaction centers (Okamura & Feher, 1992). Though ΔpK_as of 1−2 units are most commonly observed, larger shifts have been measured, for instance, in protein-based polymers (Urry et al., 1994a,b), in bacteriorhodopsin (Bashford & Gerwert, 1992), in lipases (Peters et al., 1997), for ligand (substrate/inhibitor)−enzyme complexes (Fersht & Renard, 1974; Karshikoff et al., 1993; Yamazaki et al., 1994; Swaren et al., 1995; Gordon-Beresford et al., 1996), or for active site residues (Zhang et al., 1994a; Warwicker & Gane, 1996). In bacteriorhodopsin, Asp96 and Asp115 had pK_a values higher than 7 in the calculations, but over 9 in experiments (Bashford & Gerwert, 1992). Low pK_as of active site cysteines have been observed in PTPs (Zhang et al., 1994a) or enzymes of the thioredoxin family (Warwicker & Gane, 1996). The pK_a of active site cysteine in DsbA, which catalyzes the introduction of disulfide bonds, is about 3.5 (Nelson & Creighton, 1994), as compared to that of 6.7 (Kallis & Holmgren, 1980) for the homologous thiolate in thioredoxin, which reduces disulfide bonds. Significant pK_a shifts have been determined for His134 and Lys84 in *E. coli* aspartate transcarbamylase (Villoutreix et al., 1994). The authors suggested that the low pK_as are caused by close contacts of these residues with neighboring arginines. A pK_a of 8.19 has been observed for Asp25 in HIV-1 protease upon binding of an inhibitor (Yamazaki et al., 1994). pK_a shifts of 6 units were observed for the Asp residue in protein-based polymers by increasing the number of hydrophobic residues. This was explained in terms of competition between apolar and polar groups for hydration (Urry et al., 1994b).

Evaluation of electrostatic energies in proteins dates back to the pioneering works of Linderstrom-Lang (1924), who assumed that all charges were spread uniformly over the surface of the spherical protein ("smeared-charge model"), and Tandford and Kirkwood (1957), who improved that model by considering the Coulombic interactions between the charges. The protein was considered a sphere of low dielectric constant surrounded by a high dielectric continuum representing water molecules. With the availability of crystallograhically resolved protein structures, experimentally determined pK_a data, and high-speed computers, these models have been further developed, resulting in realistic and predictive models for calculating the protonation state of titratable groups in proteins. Different refinements have been considered and successfully compared to experimental data. These improvements, for instance, include the refinement of the parameter set used in the calculations ("single site titration model") (Bashford & Karplus, 1990; Antosiewicz et al., 1994), the use of explicit water molecules (Gibas & Subramaniam, 1996), consideration of multiple conformations (Basford et al., 1993), charge changes at more than one atomic site in a given titratable group (Antosiewicz et al., 1996), the use of a high and low protein dielectric constant depending on the strength of the electrostatic interactions between titratable groups (Demchuk & Wade, 1996), and the consideration of reorganization energy (Warshel & Papazyan, 1996). In the present study, we have applied the single site titration model and have calculated the electrostatic properties of *Yersinia* PTP, PTP1B, VHR, and low molecular weight PTP to further elucidate the structural basis for the low pK_a of the active cysteine in these PTPs. The methodology of this macroscopic approach (Demchuk & Wade, 1996; Antosiewicz et al., 1994; Davis & McCammon, 1991; Davis et al., 1990; Northrup et al., 1982, 1984; McCammon & Northrup, 1981) will be briefly described in the next section.

MATERIALS AND METHODS

Materials. High-resolution crystal structures of *Yersinia* PTP, PTPB1, VHR, and low molecular weight (LMW) PTP were obtained from the Protein Data Bank at Brookhaven (Bernstein et al., 1977). Entry codes, resolutions, and references are summarized in Table 1. Hydrogens were added using CHARMm (1992). In all the calculations performed, solvent molecules, as well as ions or substrates bound to the proteins, have been removed before the

Table 1: Crystal Structures of PTPs Obtained from the Protein Data Bank at Brookhaven (Bernstein et al., 1977)[a]

structure (consensus sequence)	PDB entry code	resolution (Å)	complex with	reference
Yersinia PTP (H**C**RAGVG**R**T)	1YTW	2.5	tungstate	Fauman et al., 1996
	1YTS	2.5	sulfate	Stuckey et al., 1994; Schubert et al., 1995
	1YPT	2.5		
PTP1B (H**C**SAGIG**R**S)	2HNQ	2.8	tungstate	Jia et al., 1995; Barford et al., 1994
	1PTU	2.6	hexapeptide (DADEPYL-NH2)	
VHR (H**C**REGYS**R**S)	1VHR (2 chains)	2.1	sulfate peptidesulfonic acid	Yuvaniyama et al., 1996
LMW PTP (V**C**LGNIC**R**S)	1PHR	2.1	sulfate	Su et al., 1994; Zhang et al., 1994

[a] The active site consensus sequences for the different PTPs are given in parentheses in the first column. The active Cys and the conserved Arg are marked in boldface and are underlined.

calculations were carried out. In the 1YTS and 1PTU structures, the Ser was replaced by cysteine using the mutant structure as a template.

Electrostatic Calculations and pH Titration Procedure. The technique used to estimate the pK_as is the so-called single site titration model introduced by Bashford and Karplus (1990) and further developed by Antosiewicz et al. (1994). The computational method relies on the assumption that the ionization states of titratable amino acid side chains are exclusively electrostatic in nature. In this procedure, ionization is represented as the addition of ±1 proton charge to a single atom in each titratable group. The electrostatic field at the titrating site is calculated by numerically solving the finite difference linearized Poisson−Boltzmann equation using an incomplete Cholesky preconditioned conjugate gradient method as implemented in the UHBD program (Madura et al., 1995; Davis et al., 1990). To compute the pK_a of ionizable groups in a protein requires the evaluation of the electrostatic potentials $\psi_{i,j}$ at sites j for a unit positive charge at site i in the protein and in the model amino acids, when all partial charges of the proteins or model compounds atoms are set to zero. Having these electrostatic potentials, relative free energies $\Delta\Delta G$ are calculated:

$$\Delta\Delta G = \Delta G^{\mathrm{el}}_{\mathrm{protein}} - \Delta G^{\mathrm{el}}_{\mathrm{model}} \quad (1)$$

where $\Delta G^{\mathrm{el}}_{\mathrm{model}}$ and $\Delta G^{\mathrm{el}}_{\mathrm{protein}}$ are the electrostatic free energy differences for ionization of a given site in the model amino acid and in the protein, respectively, with all other residues neutral. For the single site protonation model the free energy differences are given by

$$\Delta G^{\mathrm{el}}_{\mathrm{model},i} = \frac{1}{2}\psi^{\mathrm{m}}_{ii} + \gamma_i \sum_{j=1}^{n} q_j \psi^{\mathrm{m}}_{ij} \quad (2)$$

$$\Delta G^{\mathrm{el}}_{\mathrm{protein},i} = \frac{1}{2}\psi^{\mathrm{p}}_{ii} + \gamma_i \sum_{j=1}^{N} q_j \psi^{\mathrm{p}}_{ij} \quad (3)$$

ψ_{ij} is the potential at the location of charge j created by a unit positive charge at site i. γ is -1 for an acidic site and $+1$ for a basic site. The superscripts m, p, n, and N refer to model amino acid, protein, number of atoms in the model compound, and number of atoms in the protein, respectively. If the neutral state of the protein is taken as the reference state, then the electrostatic energy in a given ionization state is

$$\Delta G(\mathrm{pH}, x_1, x_2, \ldots, x_{\mathrm{M}}) = 2.303RT \sum_{i=1}^{M} x_i \gamma_i (\mathrm{pH} - \mathrm{p}K_{i,\mathrm{intrinsic}}) + \sum_{i=1}^{M-1} \sum_{j=i+1}^{M} x_i x_j \gamma_i \gamma_j \psi_{ij} \quad (4)$$

where x_i is 1 when group i is ionized and 0 when it is neutral. M is the number of ionizable groups in the protein, R is the gas constant, and T is the absolute temperature. The indices i and j refer to titratable sites. p$K_{i,\mathrm{intrinsic}}$ is the intrinsic pK_a of a titratable residue, when the group is protonated in an otherwise neutral protein, and is given by

$$\mathrm{p}K_{i,\mathrm{intrinsic}} = \mathrm{p}K_{i,\mathrm{model}} - \gamma_i \Delta\Delta G_i / 2.303RT \quad (5)$$

p$K_{i,\mathrm{model}}$ = log K_a, where K_a is the equilibrium constant for association between the proton and its binding site in the model compound. Free energy differences obtained from eq 4 are used to calculate the fractional protonation for each of the M sites. The ionization state of the protein is not fixed. Due to exchange of protons with the environment, it fluctuates among all possible states with probabilities based on the Boltzmann weighting factors.

The atoms of the protein were assigned point charges and radii from the CHARMm22 force field modified by Antosiewicz et al. (1994). The radii of hydrogen atoms were set to zero, and the molecular surface was calculated with a probe of radius 1.4 Å. The dielectric constant of the solvent was $\epsilon = 80$, whereas the dielectric constant of the molecular interior was set to $\epsilon = 20$, which, in a recent study (Antosiewicz et al., 1994), has been shown to give smaller pK_a shifts and generally more accurate results for a number of proteins than calculations performed with lower dielectric constants. The relative dielectric constant was "smoothed" at the molecular surface so that it changed gradually between the protein and solvent values (Davis & McCammon, 1991). The potential was first calculated on a 45 × 45 × 45 grid with a 2 Å spacing centered on the protein. The focusing technique was then used for more exact evaluations of the potential around the ionization site by subsequently reducing the grid spacing to 1.2 Å (15 × 15 × 15 grid), 0.75 Å (15 × 15 × 15 grid), and 0.25 Å (20 × 20 × 20 grid). The protein was assumed to be surrounded by an aqueous solution of 0.15 M ionic strength with the ion density following a Boltzmann distribution at 293 K and excluded from a 2 Å thick Stern layer on the protein surface.

pK_as of the model compounds in solution were 3.8 for C-terminal carboxylate, 4.0 for Asp, 4.4 for Glu, 6.3 for His, 7.5 for the N-terminal amine, 8.3 for Cys, 9.6 for Tyr, 10.4

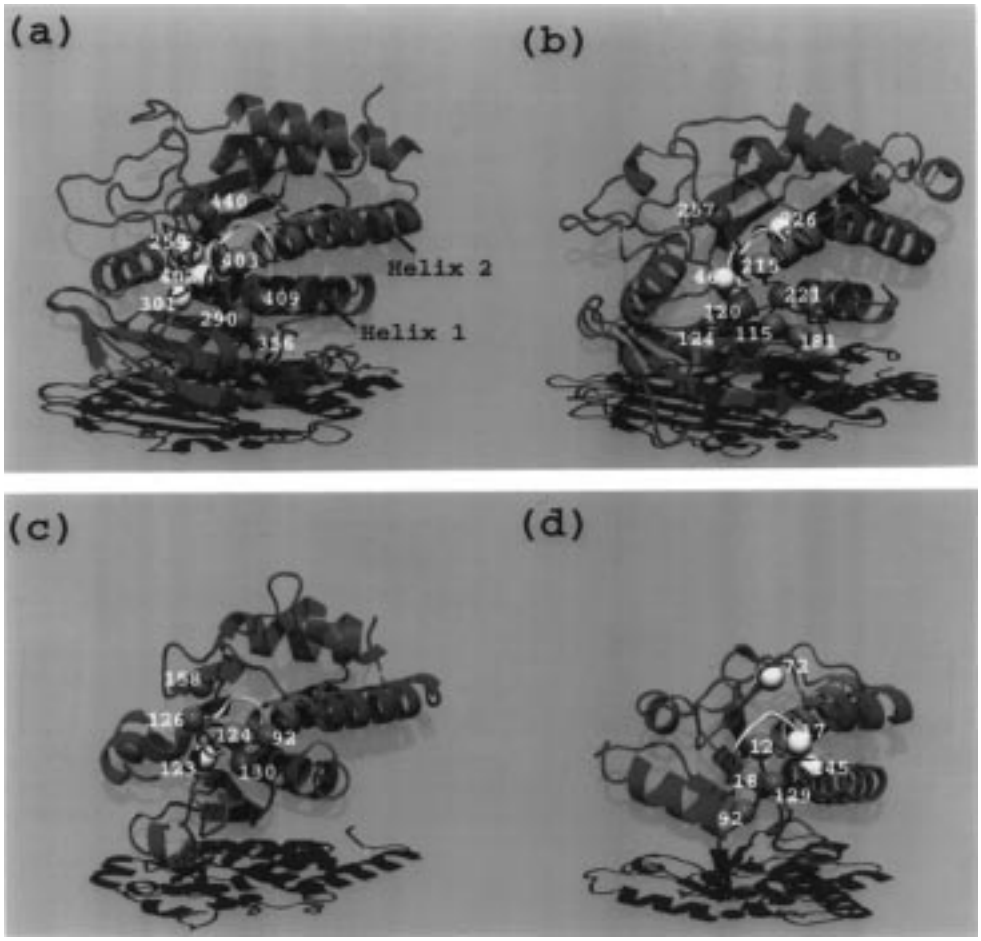

FIGURE 1: Structures of (a) *Yersinia* PTP, (b) PTP1B, (c) VHR, and (d) low molecular weight PTP. The color coding corresponds to the important components of the catalytic site. The loop in yellow comprises the active site motif [(H/V)CX_5R(S/T)]. The central α-helix is colored brown. Residues displayed in the van der Waals radius represent key interactions with the active cysteine as summarized in Table 3. Color coding is done according to their polarity: red (negative), blue (positive), and yellow (polar). The active cysteine is displayed in orange.

for Lys, and 12.0 for Arg. Ionization of these residues was modeled by a single ionizable site located at the position of the C atom in the C-terminal carboxylate group, the C^{γ} atom in Asp, the C^{δ} atom in Glu, the $N^{\epsilon 2}$ in His, the N atom in the N-terminal amine, the S^{γ} atom in Cys, the O^{η} atom in Tyr, the N^{ζ} atom in Lys, and the C^{ζ} atom in Arg (Demchuk & Wade, 1996; Antosiewicz et al., 1994).

To examine the impact of charges assigned to backbone atoms (i.e., C_{α}, C, O, N, and H), we have modified the procedure developed by Antosiewicz et al. (1994), so that the pK_a estimations can be performed with specified backbone atoms set to zero.

pK_a Estimation. To estimate the apparent pK_as, the Hybrid procedure developed by Gilson (1993) was applied. Apart from estimating the pK_as, the program also calculates charges of the protein, charges of single sites, and electrostatic energies as a function of pH. The method used in Hybrid is based on separation of ionizable groups into clusters. The interaction between ionizing charges within a cluster is treated exactly, while the intercluster interactions are approximated. This method yields both accurate energies and fractional charges of titratable sites (Gilson, 1993).

RESULTS AND DISCUSSION

Structural Comparisons. Secondary structures and sequence alignment based on structural comparison are shown in Figures 1 and 2, respectively. The color coding used in Figure 1 corresponds to the important components of the catalytic site. The loop in yellow comprises the consensus amino acid sequence [the (H/V)CX_5R(S/T) motif]. The central α-helix is colored brown. A similar color coding has been used in Figure 2, where additionally the amino acids, which are important for catalysis and not located in the P-loop, are colored red (acidic amino acid) and blue (basic residue). *Yersinia* PTP (Figure 1a) and PTP1B (Figure 1b) share only 15% sequence indentity with conserved residues, many of which are critical catalytic and substrate-binding residues. Despite low sequence homology, these structures are closely related, and as shown in Figure 1, the same overall architecture is well recognized. These structures share a highly curved, eight-stranded, mixed β-sheet flanked by two α-helices on one side and by five α-helices on the other side. VHR (Figure 1c) shares very low sequence homology with PTP1B and *Yersinia* PTP, and only 10 identical amino acids are found in the structure-based sequence alignment (Yuvaniyama et al., 1996). Most of these conserved residues are involved in phosphate binding and catalysis and, as shown below, interact strongly with the thiolate. VHR belongs to the dual-specificity protein phosphatase family and is capable of hydrolyzing phosphotyrosine, phosphothreonine, or phosphoserine residues. The specificity of these phosphatases is determined primarily by

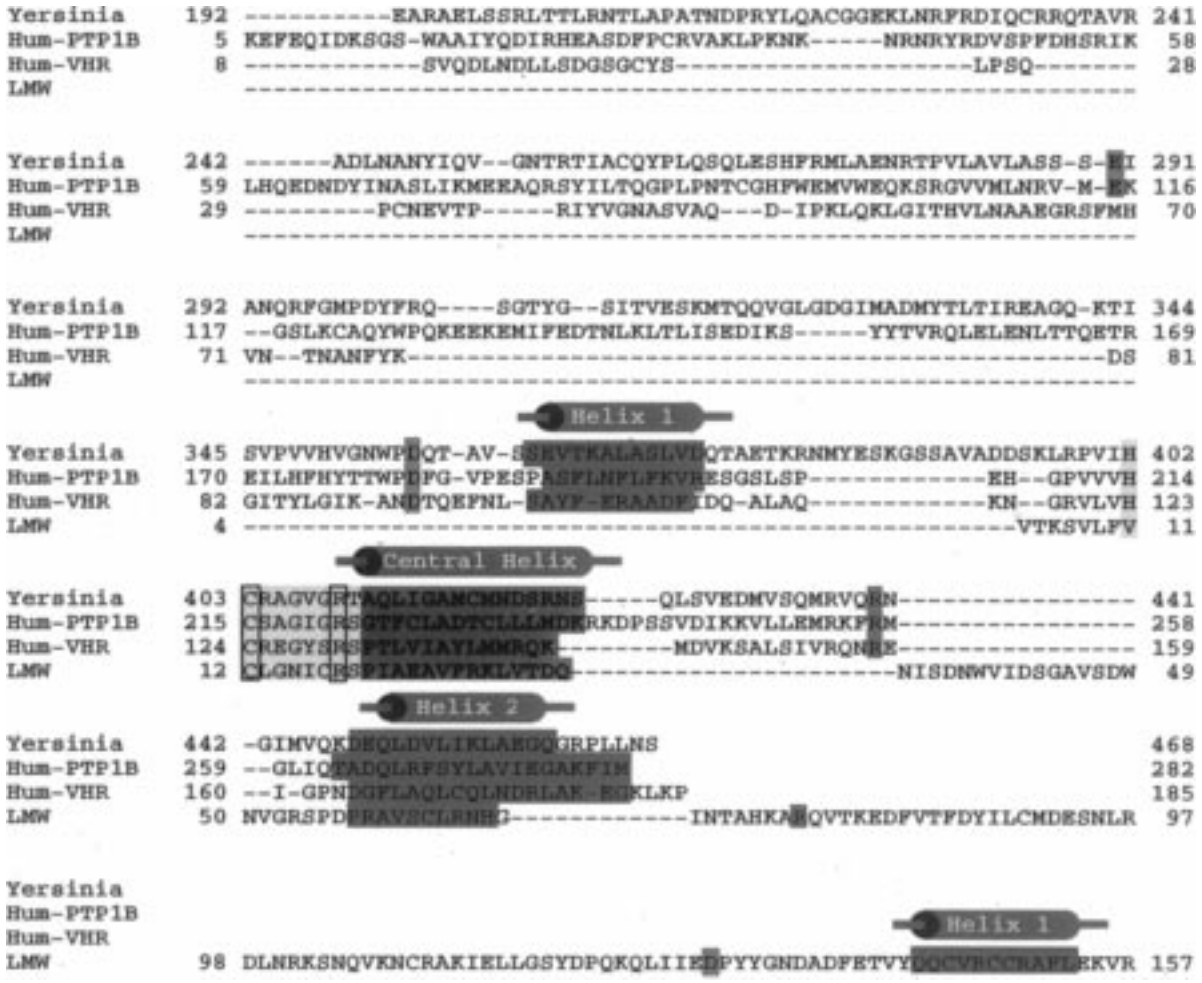

FIGURE 2: Sequence alignment based on structural comparison for *Yersinia* PTP, PTP1B, VHR, and low molecular weight PTP. The color coding corresponds to that described in Figure 1. Additionally, amino acids which are not located in the consensus sequence but important for catalysis are colored red (acidic) and blue (basic). See text for more details.

the depth of the active site cleft (Jia et al., 1995). The active site pocket of VHR is about 6 Å deep and is surrounded by side chains mainly from the P-loop itself. In contrast, the active site groove in the PTP1B and *Yersinia* PTP is approximately 9 Å deep.

In the LMW PTP (Figure 1d) only the sequence motif (H/V)CX$_5$R(S/T) is structurally and functionally equivalent to *Yersinia* PTP, PTP1B, and VHR (Figure 2). However, structural similarity is observed, and the LMW PTP has a fold that occurs in the central part of PTP1B and *Yersinia* PTP. The location of the (H/V)CX$_5$R(S/T) motif within the sequence also varies between the different phosphatases. In PTP1B and *Yersinia* PTP, the (H/V)CX$_5$R(S/T) sequence occurs toward the C-terminus of the PTP domain, whereas this motif is immediately after the N-terminus of the LMW PTP. In Figure 2, some secondary structural elements have been highlighted. The helices denoted "helix 1" and "helix 2" are found in all four structures. Interestingly, helix 1 is located in the C-terminal end of LMW PTP, a feature which is not observed in the other three PTPs.

Sensitivity of the Calculation Method. The single site titration procedure was applied to a range of PTPs. To evaluate the sensitivity of the method, we have estimated the pK_a of the titratable side chains of two different X-ray crystallographic structures of *Yersinia* PTP: (i) 1YTW (wild type, cocrystallized with tungstate) and (ii) 1YTS (active cysteine mutated to serine, cocrystallized with sulfate). Both structures were solved and analyzed in the same laboratory (Stuckey et al., 1994; Fauman et al., 1996). Prior to the electrostatic calculations using 1YTS, the serine side chain was changed to cysteine (using Quanta). The results are shown in Figure 3, where root mean square displacements (rmsd) and pK_as between the two structures are plotted vs residue number. The insert displays the pK_as (in the range from 2 to 10) of the titratable side chains obtained from the 1YTS structure vs the pK_as calculated from the 1YTW structure. Deviations from the line of identity are observed for several titratable residues (up to 1.5 pK_a units). The average deviation from the line of identity is ≈0.2. These results indicate that the method is highly sensitive to small structural differences. The same qualitative behavior is observed when pK_a values calculated for the two PTP1B structures are plotted versus each other (data not shown).

Calculation of pK_as of Active Site Cysteines. Table 2 contains the results for the calculated pK_as and the experimentally determined pK_as of the active site cysteines. It is interesting to note that for *Yersinia* PTP and PTP1B the pK_as calculated for the open structures are larger than the corresponding values calculated for the closed structures. This clearly points to the importance of the influence of conformational changes on the calculated pK_as. Recently, the population densities of the open and closed conformations

Table 2: Experimentally Determined and Computed pK_as for the Different PTPs[a]

structure	pK_a computed	conformation	pK_a exptl	reference
Yersinia PTP	5.1 (1YPT)	open	4.7	Zhang & Dixon, 1993
	4.6 (1YTW)	closed		
	4.3 (1YTS)	closed		
PTP1B	4.9 (2HNQ)	open	5.57	Lohse et al., 1997
	3.8 (1PTU)	closed		
VHR	6.3 (1VHR, chain A)		5.6	Denu & Dixon, 1995
	6.0 (1VHR, chain B)			
LMW PTP	6.7 (1PHR)		<4, 6.7	Evans et al., 1996; Zhang et al., 1992

[a] The PDB entry codes are given in parentheses.

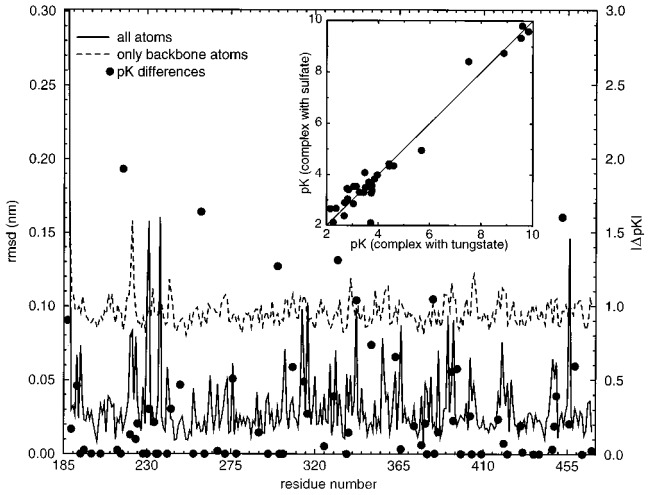

FIGURE 3: Examples illustrating the sensitivity of the single site titration method. Root mean square displacements (rmsd) (left coordinate) and pK_as (right coordinate) calculated between the two X-ray crystallographic structures of *Yersinia* PTP in the active form crystallized with different ions bound to the active site. The insert shows the pK_as of the titratable groups calculated for the 1YTW structure vs the 1YTS structure.

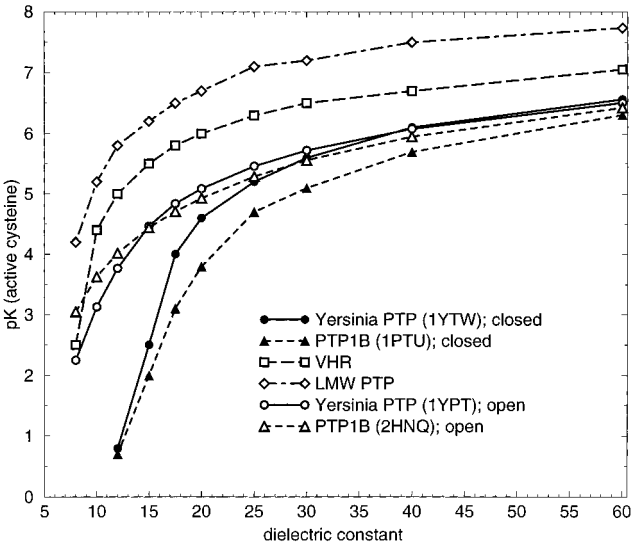

FIGURE 4: Computed pK_a of the active cysteine as a function of dielectric constant for the different phosphatases.

of *Yersinia* PTP were investigated (Juszczak et al., 1997), revealing that the two conformations are equally populated. Therefore, the average values of the calculated pK_as for the open and closed conformations (i.e., 4.8 for *Yersinia* PTP and 4.4 for PTP1B) should be compared to the experimentally determined pK_as [i.e., 4.7 for *Yersinia* PTP and 5.57 for PTP1B (Table 2)]. Good agreement is observed for *Yersinia* PTP and VHR, and the observed deviations are within the experimental error (Denu & Dixon, 1995; Zhang & Dixon, 1993). In the case of LMW PTP two experimental observations have been reported (pK_a <4 and pK_a 6.7; see Table 2), where the larger value matches the calculated pK_a. For PTP1B the calculated pK_a values are more than 1 unit below that experimentally determined. This discrepancy could be due to the simplicity of the model, and there are several possible sources of error in these calculations. The flexibility of the enzyme could allow a large range of electrostatic environments to a titrating site, and hence, conformational changes could be coupled to the titration behavior (Bashford et al., 1993; Warshel & Åqvist, 1991) as seen in the case of *Yersinia* PTP and PTP1B. Further, the representation of water as a continuum, which neglects, for instance, a protein-bound water molecule acting as a hydrogen-bonding bridge between two titratable groups, might result in wrong estimation of the pK_as. Another possible source of deviations is the binding of counterions to specific sites in the enzyme structures. It is expected that the model breaks down for strongly interacting ionizable groups, where polarizability of these residues plays an important role (Holst et al., 1994; Bashford & Karplus, 1990). To further elucidate the magnitude of the electrostatic interactions, calculations were performed at different dielectric constants. The resulting pK_as of the active cysteine versus the dielectric constant are displayed in Figure 4. It appears that the pK_as for the active cysteine are more strongly dependent on the dielectric constant in the closed conformations of *Yersinia* PTP and PTP1B than in the corresponding open conformations. Furthermore, the inherently open structures, VHR and LMW PTP, show qualitatively the same behavior as observed for the open conformations of *Yersinia* PTP and PTP1B. Generally, it is noticeable that the pK_as of the active cysteines are several units below the value determined for a free cysteine amino acid residue. This indicates that the pK_as of the cysteines are perturbed by the interactions between the active cysteine and charges in the vicinity of the active site. These interactions may originate (i) from the partial charges assigned to polar atoms to model the effect of dipoles and hydrogen bond capacities or (ii) from charges assigned to ionizable side chains. The influence of neighboring charges will be discussed below.

Influence of Backbone Charges on Active Site pK_as. To explore the factors that contribute to the unusually low pK_a value of the active site cysteines, we have examined the influence of the protein backbone charges (i.e., the charges assigned to the polar atoms C_α, C, O, N, and H) on the pK_a. These partial charges were set to zero in a systematic way for all the PTPs studied using the following procedure: The

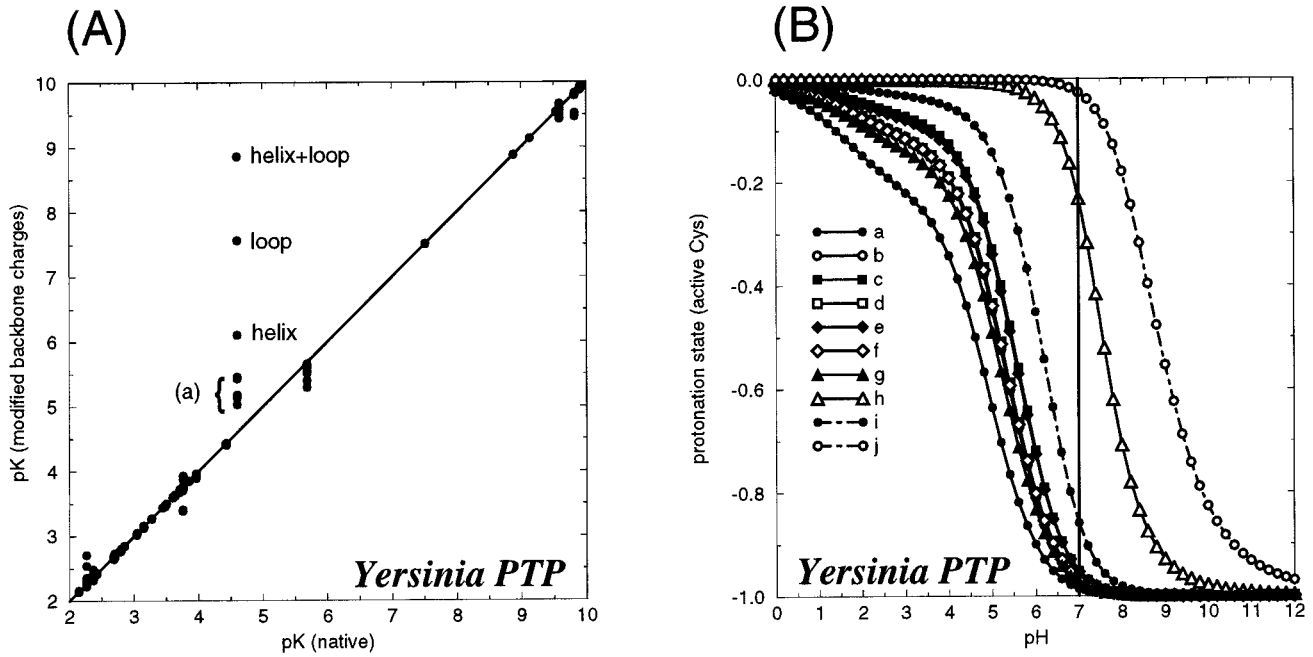

FIGURE 5: Titration results for the *Yersinia* PTP. (A) pK_as computed with modified backbone charges as a function of pK_as in the native PTP. (a) marks the pK_a shifts when backbone charges of individual residues in the loop are sequentially zeroed. Loop indicates the pK_a shift when the backbone charges of all residues in the loop are zeroed. Helix marks the pK_a shift when the backbone charges of all amino acids in the central α-helix are zeroed. Helix + loop indicates that backbone charges of all residues in the loop and central α-helix are zeroed. (B) Protonation of the active cysteine as a function of pH for (a) native PTP, (b−g) backbone charges of individual residues in the loop sequentially zeroed, (h) backbone charges of all residues in the loop zeroed, (i) backbone charges of all amino acids in the central α-helix zeroed, and (j) backbone charges of all amino acids in the loop and central α-helix zeroed.

partial charges of the backbone atoms for each amino acid constituting the consensus sequence were consecutively set to zero [labeled (a) in Figures 5A−8A], all the backbone charges of the consensus sequence were set to zero (labeled loop in Figures 5A−8A), all the backbone charges in the central α-helix were set to zero (labeled helix in Figures 5A−8A), and finally, all backbone charges in both the consensus sequence and the central α-helix were set to zero (labeled loop + helix in Figures 5A−8A). The influence of these charge changes on pK_as was then evaluated. To further analyze the impact of the permanent backbone charges on the pK_as, the pK_a of the active site cysteine was studied as a function of pH for the four models described above (Figures 5B−8B).

In Figure 5 the results obtained for the *Yersinia* PTP are shown. In Figure 5A, the pK_as calculated after the backbone charges were perturbed (as described above) have been mapped vs the pK_as calculated without any perturbations. pK_as of all titratable side chains within the range from 2 to 10 are shown in Figure 5A. The only side chain which is significantly influenced by the charge perturbations is the active site cysteine. The pK_a of the cysteine in the unperturbed case is 4.6 (see Table 2, 1YTW). The impact of charge perturbations on the pK_a of the other titratable side chains is smaller than what is observed for different X-ray crystallographic structures of the same enzyme (see Figure 3). The case denoted (a) shows a slight increase of active site cysteine pK_a. In the model helix, which corresponds to cancellation of the electrostatic dipole generated by the backbone charges of the central α-helix, the pK_a increases further (pK_a = 6.1). This increase in the pK_a (i.e., destabilization of the thiolate form) is consistent with the picture of a macroscopic α-helix dipole, which has its positive pole at the N-terminus and its negative pole at the C-terminus of the helix (Wada, 1976; Knowles, 1991). It has been shown that the electric field generated by the helix dipole moment has a general function in proteins, for instance, enhancing the binding of negatively charged groups, altering the nucleophilic character of side chains located near the N-terminus, and stabilizing charged transition states along the catalytic pathways (Hol et al., 1978, 1981; Åqvist et al., 1991). Combining the effect of the consensus loop backbone charges (case loop) gives an increase which is more significant (pK_a = 7.6) than the influence of the central α-helix (pK_a = 6.1). Finally, combining the effect of the backbone charges in the loop as well as in the helix gives a shift to a value which is above the intrinsic value for cysteine. The combined effect results in a pK_a equal to 8.9. This observation strongly suggests that in the case of *Yersinia* PTP the secondary structures comprised by the consensus sequence loop and the central α-helix cause the low pK_a of the active site cysteine.

To further explore the generality of this observation, the three other PTPs considered above have been examined using the same procedure as for *Yersinia* PTP. In Figures 6−8, the results obtained for PTP1B, VHR, and LMW PTP are shown. The same general tendency, as found for the *Yersinia* PTP, is observed for the other three PTPs. The structural arrangement of the consensus loop and the central α-helix generate a sufficiently strong electrostatic field, which stabilizes the thiol anion. This is in agreement with the earlier experimental observation that the thiolate is stabilized by an extensive network of hydrogen bonds between the backbone NH of the consensus loop and the active cysteine (Stuckey et al., 1994; Stunnenberg, 1993). Our results indicate that the accumulation of backbone microdipoles

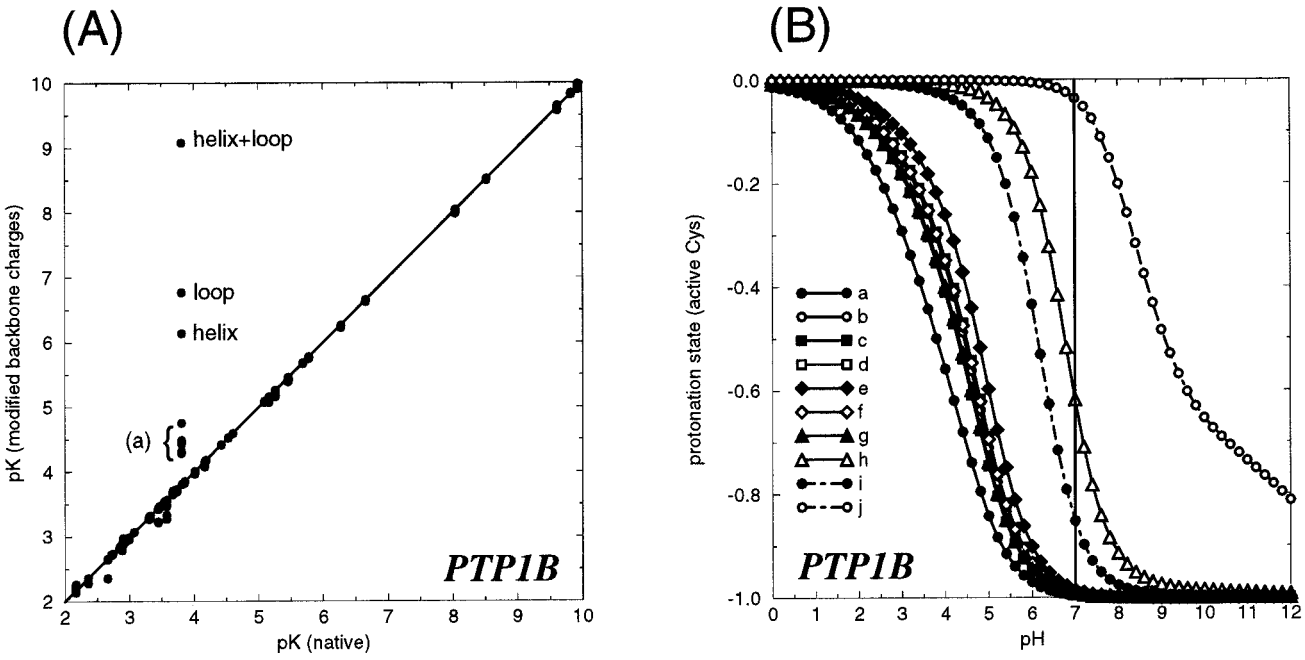

FIGURE 6: Titration results for the PTP1B. See caption to Figure 5 for more details.

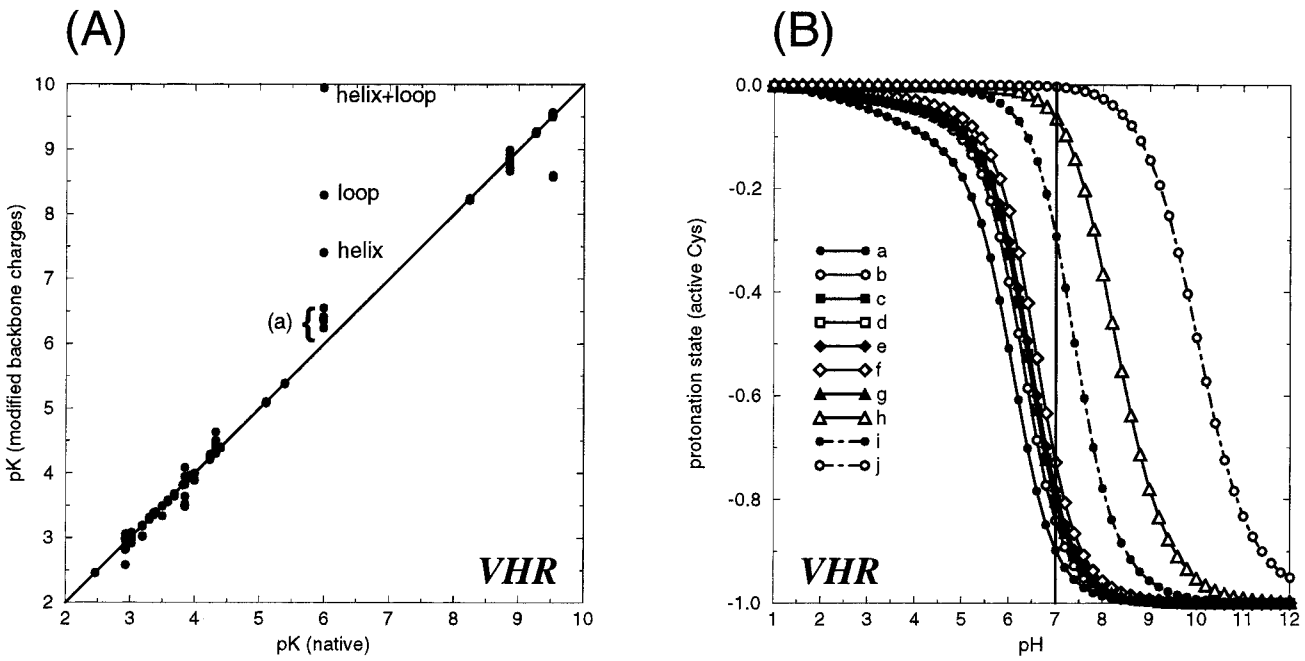

FIGURE 7: Titration results for the VHR. See caption to Figure 5 for more details.

generated by the consensus sequence amino acids has a larger impact on the pK_a of the active site cysteine than the electrostatic dipole generated by the central α-helix.

For an estimation of the magnitude of the electrostatic field in the binding pocket of the four different PTPs, we have computed the pH titration of the active site cysteine as a function of pH. The titration curves shown in Figures 5B−8B have the typical S-shaped characteristics describing a smooth transition from the neutral to the thiolate state. This behavior indirectly indicates that the electrostatic forces in the binding pocket are relatively weak. It has been shown that as the interaction energy between sites increases, the fraction ionized increases more slowly, effectively buffering the system from changes in the protein environment (Yang et al., 1993). Deviations from the typical S-shaped curve were observed for interactions greater than approximately 3 kcal/mol (Yang et al., 1993).

In Figure 9 the $\Delta(\Delta G)$s resulting from changes in backbone charges are shown. A consistent pattern is observed when the results from the four different PTPs are compared. Generally, it is observed that the contribution from each peptide bond is comparable and that the major contribution stems from the backbone atoms in the consensus loop.

Influence of Other Charges on the Active Site pK_a. According to the results in the preceding section, stabilization of the ionized form of the active site cysteine primarily originates from the charges assigned to the polar backbone atoms. However, several studies have revealed that mutations of residues in the P-loop significantly reduce the activity

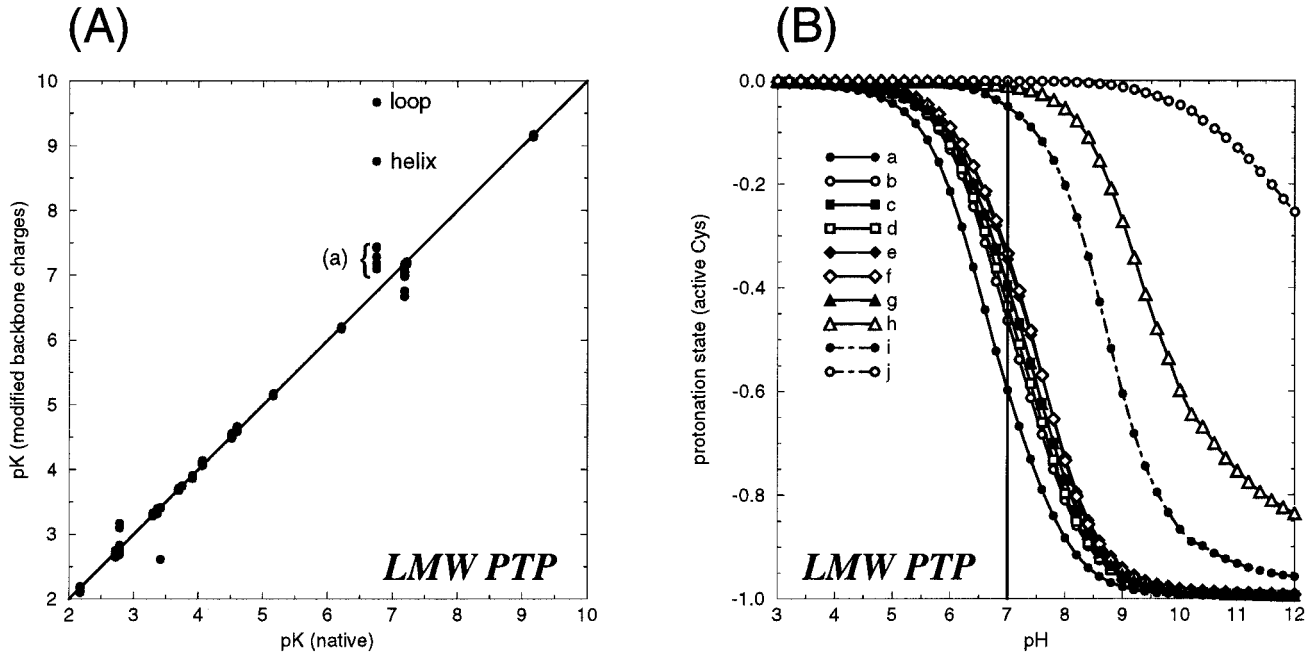

FIGURE 8: Titration results for the low molecular weight PTP. See caption to Figure 5 for more details.

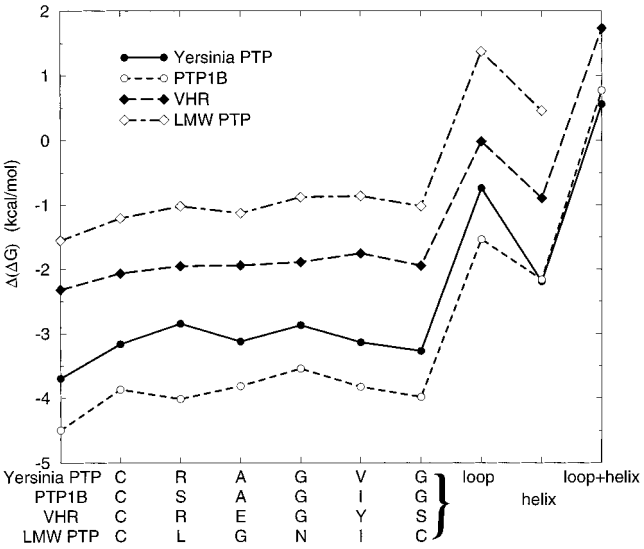

FIGURE 9: $\Delta(\Delta G)$ values for different treatment of the backbone charges. The residue identification (*x*-axis, one letter code) starting at the active cysteine indicates which backbone charge is zeroed in the calculation. See caption to Figure 5 for more details.

of the enzyme (Evans et al., 1996). It has been suggested that the activity loss is mainly due to the disruption of the hydrogen-bonding network and that these residues in the native enzyme predominately serve structural functions that allow the active site to adopt an optimal geometry for phosphate binding.

To investigate the role of the Ser (in PTP1B, VHR, LMW PTP) and Thr (in *Yersinia* PTP) at the position just after the conserved arginine, we have mutated these residues with Ala and calculated the pK_a of the active Cys. Overall, we observe that mutation of Ser/Thr to Ala reduces the pK_as of the active cysteine. For the different phosphatases the pK_as and $\Delta(\Delta G)$s (given in parentheses) are 3.1 (−5.2) for the closed conformation of *Yersinia* PTP, 5.1 (−3.2) for the open conformation of *Yersinia* PTP, 3.1 (−5.2) for the closed conformation of PTP1B, 4.3 (−4.0) for the open conformation of PTP1B, 5.7 (−2.6) for VHR, and 6.4 (−1.9) for the LMW PTP. This would suggest that this mutation stabilizes the thiolate. Recently, Hansen et al. (1997) used computational techniques to investigate the proton transfer between the active Cys12 in LMW PTP and a phenyl phosphate ion and to study the effect of the Ser19 to Ala mutation on the charge state of the active Cys. Their results indicated that the architecture of the enzyme as well as the Ser stabilizes the thiolate anion form of the catalytic cysteine. Hansen et al. (1997) studied the bound complex, whereas the present study focuses on the electrostatic properties of the enzyme alone. Considering both results suggests that the Ser/Thr residues serve two functions. In the uncomplexed form the Ser/Thr residues destabilize the thiolate form and probably support the binding of the phosphate moiety. Upon binding of the charged phosphate group, the electrostatic field around the active Cys changes and the Ser may have an additional purpose of stabilizing the thiolate form.

To evaluate the influence of titratable charges on the pK_a of the active cysteine, we have determined the electrostatic interaction energies between the active cysteine and other ionizable residues. The results are summarized in Table 3, where interaction pairs and electrostatic interaction energies (greater than 0.59 kcal/mol, corresponding to *kT* at 293 K) are listed. Note that a positive interaction energy stabilizes the thiolate form (decreases the pK_a), while a negative value destabilizes the thiolate form (increases the pK_a). As suggested by site-directed mutagenesis (Eckstein et al., 1996; Fauman & Saper, 1996; Barford, 1995), the two residues, an arginine (from the consensus motif) and an aspartic acid, which are absolutely conserved in the four phosphatase families have strong interactions with the active cysteine. The conserved aspartic acid is Asp356 in *Yersinia* PTP, Asp181 in PTP1B, Asp92 in VHR, and Asp129 in LMW PTP. However, the effects on the pK_a of the active Cys are opposing; the arginine stabilizes the thiolate form while the aspartate destabilizes the thiolate form. In general, the overall net effect of the titratable charges on the pK_a of the

Table 3: Interactions between the Active Cysteine and Residues Whose Interaction Energies Are Greater than 0.59 kcal/mol

structure	active Cys	interaction with	energy (kcal/mol)	pK_a shift
Yersinia PTP (1YTW)	Cys403	Arg409	+2.17	1.62
		Asp356	−1.03	0.77
		His402	+0.92	0.69
		Arg440	+0.92	0.68
		Glu290	−0.90	0.67
		Cys259	−0.84	0.63
		Tyr301	−0.59	0.44
PTP1B (1PTU)	Cys215	Arg221	+2.20	1.64
		Asp181	−1.31	0.98
		Arg257	+1.11	0.83
		His214	+0.99	0.74
		Cys226	−0.91	0.68
		Glu115	−0.84	0.63
		Tyr46	−0.73	0.55
		Cys121	−0.71	0.53
		Tyr124	−0.61	0.45
		Lys120	+0.59	0.44
VHR (1VHR, chain A)	Cys124	Arg130	+1.65	1.23
		Asp92	−0.93	0.69
		Arg158	+0.89	0.67
		His123	+0.88	0.66
		Glu126	−0.68	0.51
LMW PTP (1PHR)	Cys12	Arg18	+1.76	1.31
		Cys17	−1.56	1.16
		Asp129	−1.10	0.82
		His72	+0.74	0.55
		Cys145	−0.69	0.51
		Asp92	−0.62	0.46

active cysteine is negligible because the charges tend to cancel each other.

There are only 10 identical amino acids (including the active cysteine) found in *Yersinia* PTP, PTP1B, and VHR. Seven of these amino acids are titratable, and five of these residues have strong interactions with the active cysteine (see Table 3), although the accumulated effect is negligible. Interestingly, an arginine (Arg75) is present in the LMW PTP, which is equivalent to Arg440 (in *Yersinia* PTP), Arg257 (in PTP1B), and Arg158 (in VHR) (these arginines are colored blue in the sequence alignment; Figure 2). But, in contrast to these arginines, Arg75 only weakly interacts with the active cysteine (<0.59 kcal/mol). It is notable that both VHR and LMW PTP have an ionizable residue in the P-loop (Glu126 in VHR and Cys17 in LMW PTP). This pattern is not found in *Yersinia* PTP and PTP1B.

CONCLUSION

Protein−tyrosine phosphatases (PTPs) belong to growing families of enzymes which are involved in the regulation of a variety of cellular events. The current estimate is that humans have as many as 1000 phosphatase genes, and many phosphatases show high selectivity and specificity. To further elucidate the structure−function relationship of phosphatases, we have investigated the electrostatic properties of *Yersinia* PTP, PTP1B, VHR, and LMW PTP in the vicinity of the active site. We have applied a macroscopic approach based on the Poisson−Boltzmann description of the protein−solvent system (Demchuk & Wade, 1996; Antosiewicz et al., 1994; Bashford & Karplus, 1990) to examine the influence of the charge distribution in the binding pocket on the protonation state of the active site cysteine. The estimated pK_as of the active site cysteines in *Yersinia* PTP, PTP1B, VHR, and LMW PTP are in reasonable agreement with the experimentally determined pK_as. By averaging the results obtained for the open and closed conformations of *Yersinia* PTP and PTP1B, better agreement between the calculated and experimentally determined pK_as is obtained. This is in accordance with the recent investigation of the dynamics of the active site lid in *Yersinia* PTP (Juszczak et al., 1997), where it has been shown that both the open and closed conformations are equally populated. Analysis of the charges contributing to the pK_a shift shows that the net influence of titratable charges is negligible. The major contribution as has been suggested earlier for *Yersinia* PTP (Stuckey et al., 1994) comes from the electrostatic microdipoles created by the backbone charges (i.e., the $CONHC_\alpha$ atoms) of the consensus sequence $(H/V)CX_5R(S/T)$. Due to the very peculiar loop conformation, these microdipoles all point in the direction of the thiol atom of the active site cysteine giving a major contribution to the pK_a shift. Another important contribution comes from the electrostatic dipole generated by the backbone charges of the central α-helix, in which the cysteine is positioned N-terminally. The results in the present investigation point to the importance of the conserved structural elements consisting of the consensus sequence loop and a central α-helix, which both seem responsible for the unusually low pK_a of the catalytically active cysteines. However, the former structural element has a greater impact on the pK_a shift. Despite the low sequence homology among protein−tyrosine phosphatases structurally conserved elements stabilize the thiolate anion (Evans et al., 1996; Stuckey et al., 1994).

ACKNOWLEDGMENT

Helpful discussions with J. Antosiewicz, E. Fauman, M. Saper, and Z.-Y. Zhang are acknowledged.

REFERENCES

Antosiewicz, J., McCammon, J. A., & Gilson, M. K. (1994) *J. Mol. Biol. 238*, 415−436.
Antosiewicz, J., McCammon, J. A., & Gilson, M. K. (1996) *Biochemistry 35*, 7819−7833.
Åqvist, J., Luecke, H., Quiocho, F. A., & Warshel, A. (1991) *Proc. Natl. Acad. Sci. U.S.A. 88*, 2026−2030.
Auzat, I., & Garel, J.-R. (1992) *Protein Sci. 1*, 254−258.
Barford, D. (1995) *Curr. Opin. Struct. Biol. 5*, 728−734.
Barford, D., Flint, A. J., & Tonks, N. K. (1994) *Science 263*, 1397−1404.
Bashford, D., & Karplus, M. (1990) *Biochemistry 29*, 10219−10255.
Bashford, D., & Gerwert, K. (1992) *J. Mol. Biol. 224*, 473−486.
Bashford, D., Case, D. A., Dalvit, C., Tennant, L., & Wright, P. E. (1993) *Biochemistry 32*, 8045−8056.
Bernstein, F. C., Koetzle, T. F., Williams, G. J. B., Meyer, E. F., Brice, M. D., Rogers, J. R., Kennard, O., Shimanouchi, T., & Tasumi, M. (1977) *J. Mol. Biol. 112*, 535−542.
Bilwes, A. M., den Hertog, J., Hunter, T., & Noel, J. P. (1996) *Nature 382*, 555−559.
CHARMm Molecular Modeling Software Package, Release 3.3 (1992) Molecular Simulations Inc., 200 Fifth Ave., Waltham, MA 02154.
Courtneidge, S. A. (1994) *Semin. Cancer Biol.*, 239−246.
Cox, S., Radzio-Andzelm, E., & Taylor, S. S. (1994) *Curr. Opin. Struct. Biol. 4*, 893−901.
Dao-pin, S., Anderson, D. E., Baase, W. A., Dahlquist, F. W., & Matthews, B. W. (1991) *Biochemistry 30*, 11521−11529.
Davis, M. E., & McCammon, J. A. (1991) *J. Comput. Chem. 7*, 909−912.

Davis, M. E., Madura, J. D., Luty, B. A., & McCammon, J. A. (1990) *Comput. Phys. Commun. 62*, 187−197.
Demchuk, E., & Wade, R. C. (1996) *J. Phys. Chem. 100*, 17373−17387.
Denu, J. M., & Dixon, J. E. (1995) *Proc. Natl. Acad. Sci. U.S.A. 92*, 5910−5914.
Eckstein, J. W., Beer-Romero, P., & Berdo, I. (1996) *Protein Sci. 5*, 5−12.
Evans, B., Tishmack, P. A., Pokalsky, C., Zhang, M., & Van Etten, R. L. (1996) *Biochemistry 35*, 13609−13617.
Fauman, E. B., & Saper, M. A. (1996) *Trends in Biochem. Sci. 21*, 413−417.
Fauman, E. B., Yuvaniyama, C., Schubert, H. L., Stuckey, J. A., & Saper, M. A. (1996) *J. Biol. Chem. 271*, 18780−18788.
Fersht, A. R., & Renard, M. (1974) *Biochemistry 13*, 1416−1426.
Fisher, E. H., Charbonneau, H., & Tonks, N. K. (1991) *Science 253*, 401−406.
Gibas, C. J., & Subramaniam, S. (1996) *Biophys. J.*, 138−147.
Gilson, M. K. (1993) *Proteins: Struct., Funct. Genet. 15*, 266−282.
Gordon-Beresford, R. M. H., Belle, D. V., Giraldo, J., & Wodak, S. J. (1996) *Proteins: Struct., Funct. Genet. 25*, 180−194.
Hansson, T., Nordlund, P., & Åqvist, J. (1997) *J. Mol. Biol. 265*, 118−127.
Hol, W. G. J., Van Duijnen, P. T., & Berendsen, H. J. C. (1978) *Nature 273*, 443−446.
Hol, W. G. J., Halie, L. M., & Sander, C. (1981) *Nature 294*, 532−536.
Holst, M., Kozack, R. E., Saied, F., & Subramaniam, S. (1994) *Proteins: Struct., Funct., Genet. 18*, 231−245.
Honig, B., & Nicholls, A. (1995) *Science 268*, 1144−1149.
Hunter, T. (1995) *Cell 80*, 225−235.
Inoue, M., Yamada, H., Yasukochi, T., Kuroki, R., Miki, T., Horiuchi, T., & Imoto, T. (1992) *Biochemistry 31*, 5545−5553.
Jackson, S. E., & Fersht, A. R. (1993) *Biochemistry 32*, 13909−13916.
Jia, Z., Barford, D., Flint, A. J., & Tonks, N. K. (1995) *Science 268*, 1754−1758.
Juszczak, L. J., Zhang, Z.-Y., Wu, L., Gottfried, D. S., & Eads, D. D. (1997) *Biochemistry 36*, 2227−2236.
Kallis, G. B., & Holmgren, A. (1980) *J. Biol. Chem. 255*, 10261−10265.
Karshikoff, A., Reinemer, P., Huber, R., & Ladenstein, R. (1993) *Eur. J. Biochem. 215*, 663−670.
Khorana, H. G. (1993) *Proc. Natl. Acad. Sci. U.S.A. 90*, 1166−1171.
King, G., Lee, F. S., & Warshel, A. (1991) *J. Chem. Phys. 95*, 4366−4377.
Knowles, J. R. (1991) *Nature 350*, 121−124.
Langetsmo, K., Fuchs, J. A., & Woodward, C. (1991a) *Biochemistry 30*, 7603−7609.
Langetsmo, K., Fuchs, J. A., Woodward, C., & Sharp, K. A. (1991b) *Biochemistry 30*, 7609−7614.
Levitzki, A., & Gazit A. (1995) *Science 267*, 1782−1788.
Linderstrom-Lang, K. (1924) *Cr. Trav. Lab. Carlsberg 15*, 1−29.
Lohse, D. L., Denu, J. M., Santoro, N., & Dixon, J. E. (1997) *Biochemistry 36*, 4568−4575.
Madura, J. D., Briggs, J. M., Wade, R. C., Davis, M. E., Luty, B. A., Ilin, A., Antosiewicz, J., Gilson, M. K., Bagheri, B., Scott, L. R., & McCammon, J. A. (1995) *Comput. Phys. Commun. 91*, 57−67.
McCammon, J. A., & Northrup, S. H. (1981) *Nature 293*, 316−317.
McGrath, M. E., Vasquez, J. R., Craik, C. S., Yang, A. S., Honig, B., & Fletterick, R. J. (1992) *Biochemistry 31*, 3059−3064.
Nelson, J. W., & Creighton, T. E. (1994) *Biochemistry 33*, 5974−5983.
Northrup, S. H., Zarin, F., & McCammon, J. A. (1982) *J. Phys. Chem. 86*, 2314−2321.
Northrup, S. H., Allinson, S. A., & McCammon, J. A. (1984) *J. Chem. Phys. 80*, 1517−1524.
Okamura, M. Y., & Feher, G. (1992) *Annu. Rev. Biochem. 61*, 861−896.
Peters, G. H., Toxvaerd, S., Olsen, O. H., & Svendsen, A. (1997) *Protein Eng. 10*, 137−147.
Pot, D. A., & Dixon, J. E. (1992) *Biochim. Biophys. Acta 1136*, 35−43.
Rodrigues, G. A., & Park, M. (1994) *Curr. Opin. Genet. Dev. 4*, 15−24.
Saito, H. (1993) *Cell Biol. 4*, 379−387.
Schubert, H. L., Fauman, E. B., Stuckey, J. A., Dixon, J. E., & Saper, M. A. (1995) *Protein Sci. 4*, 1904−1913.
Stone, R. L., & Dixon, J. E. (1994) *J. Biol. Chem. 269*, 31323−31326.
Stuckey, J. A., Schubert, H. L., Fauman, E. B., Zhang, Z.-Y., Dixon, J. E., & Saper, M. A. (1994) *Nature 370*, 571−574.
Stunnenberg, H. (1993) *Bioessays 15*, 309−315.
Su, X.-D., Taddei, N., Stefani, M., Ramponi, G., & Nordlund. P. (1994) *Nature 370*, 575−578.
Swaren, P., Maveyraud, L., Guillet, V., Masson, J.-M., Mourey, L., & Samama, J.-P. (1995) *Structure 3*, 603−613.
Tandford, C., & Kirkwood, J. G. (1957) *J. Am. Chem. Soc. 79*, 5333−5339.
Urry, D. W., Gowda, D. C., Peng, S., Parker, T. M., Jing, N., & Harris, R. D. (1994a) *Biopolymers 34*, 889−896.
Urry, D. W., Peng, S., Gowda, D. C., Parker, T. M., & Harris, R. D. (1994b) *Chem. Phys. Lett. 225*, 97−103.
Villoutreix, B. O., Spassov, V. Z., Atanasov, B. P., Herve, G., & Ladjimi, M. M. (1994) *Proteins: Struct., Funct., Genet. 19*, 230−243.
Wada, A. (1976) *Adv. Biophys. 9*, 1−63.
Warshel, A., & Åqvist, J. (1991) *Annu. Rev. Biophys. Biophys. Chem. 20*, 267−298.
Warshel, A., & Papazyan, A. (1996) *Proc. Natl. Acad. Sci. U.S.A. 93*, 13665−13670.
Warwicker, J., & Gane, P. J. (1996) *FEBS Lett. 385*, 105−108.
Wells, J. A., Powers, D. A., Bott, R. R., Graycar, T. P., & Estell, D. A. (1987) *Proc. Natl. Acad. Sci. U.S.A. 84*, 1219−1223.
Yamazaki, T., Nicholson, L. K., Torchia, D. A., Wingfield, P., Stahl, S. J., Kaufman, J. D., Eyermann, C. J., Hodge, C. N., Lam, P. Y. S., Ru, Y., Jadhav, P. K., Chang, C.-H., & Weber, P. C. (1994) *Proc. Natl. Acad. Sci. U.S.A. 116*, 10791−10792.
Yang, A.-S., Gunner, M. R., Sampogna, R., Sharp, K., & Honig, B. (1993) *Proteins: Struct., Funct., Genet. 15*, 252−265.
Yuvaniyama, J., Denu, J. M., Dixon, J. E., & Saper, M. A. (1996) *Science 272*, 1328−1331.
Zhang, Z. Y., & Dixon, J. E. (1993) *Biochemistry 32*, 9340−9345.
Zhang, Z. Y., Davis, J. P., & Etten, R. L. V. (1992) *Biochemistry 31*, 1701−1711.
Zhang, M., Etten, R. L. V., & Stauffacher, C. V. (1994) *Biochemistry 33*, 11097−11105.
Zhang, Z. Y., Maclean, D., McNamara, D. J., Sawyer, T. K., & Dixon, J. E. (1994a) *Biochemistry 33*, 2285−2290.
Zhang, Z. Y., Wang, Y., & Dixon, J. E. (1994b) *Proc. Natl. Acad. Sci. U.S.A. 91*, 1624−1627.

BI971187I